

Lowpass FSS for 50-230 GHz Quasi-Optical Demultiplexing for the MetOp Second Generation Microwave Sounder Instrument

Raymond Dickie *Senior Member IEEE*, Steven Christie, Robert Cahill *Senior Member IEEE*, Paul Baine, Vincent Fusco *Fellow IEEE*, Kai Parow-Souchon, Manju Henry, Peter G. Huggard *Senior Member IEEE*, Robert S. Donnan, Oleksandr Sushko, Massimo Candotti, Rostyslav Dubrovka, Clive G. Parini and Ville Kangas

Abstract— This paper reports the design, manufacture and characterisation of a new frequency selective surface (FSS) structure which meets the demanding requirements for transmission of 50.2 – 57.7 GHz radiation simultaneously for TE and TM polarizations at 45° incidence, and reflection of signals in four discrete higher frequency bands centered at 89 GHz, 165.5 GHz, 183.3 GHz and 229 GHz. The FSS is required for a quasi-optical network, which was developed during preparatory breadboarding of the Microwave Sounder instrument. The 100 mm diameter ultra-wide band FSS must exhibit ≤ 0.25 dB loss for all signals in the above bands, and has to satisfy the requirements of the space environment. The FSS is formed by a periodic metal film array sandwiched between two 0.83 mm thick, optically flat, fused quartz substrates. It has 19,000 unit cells composed of two compact resonant slot elements, a meandering elliptical annulus and a folded dipole. Spectral transmission and reflection measurements in the 50 – 230 GHz frequency range yielded results that are in excellent agreement with numerical predictions.

Index Terms—Dichroic filters, Earth observation instruments, frequency selective surfaces (FSS), micromachined structures, quasi-optical technology

I. INTRODUCTION

THE MicroWave Sounder (MWS) radiometer is a spaceborne across-track scanning instrument [1], [2], that provides measurements of temperature profiles, water vapour profiles and information on cloud liquid water, key input parameters for numerical weather prediction [3]. To satisfy

Manuscript received December 15, 2016, “This work was supported by the European Space Agency (ESA) under Contract 4000107540/12/NL/BJ”.

R. Dickie, R. Cahill, P. Baine and V. Fusco are with the Institute of Electronics, Communications and Information Technology, Queen’s University Belfast, Belfast BT3 9DT Northern Ireland, UK, (e-mail: r.dickie@qub.ac.uk)

S. Christie is with Arralis Technologies Ltd, Queen’s Road, Belfast, BT3 9DT, UK.

R. S. Donnan, O. Sushko, M. Candotti, R. Dubrovka & C. G. Parini are with the School of Electronic Engineering and Computer Science, Queen Mary University of London, Peter Landin Building, 10 Godward Square, London E1 4FZ, UK. O. Sushko is now with Radioengineering department, Igor Sikorsky Kyiv Polytechnic Institute, 37 Peremohy Ave. Kyiv, Ukraine, 03056.

K. Parow-Souchon, M. Henry and P. G. Huggard, are with RAL Space, STFC Rutherford Appleton Laboratory, Didcot OX11 0QX, UK.

V. Kangas is with Earth Observation Projects Department (EOP-PIM), European Space Agency / ESTEC, P.O.Box299, 2200AG Noordwijk ZH, The Netherlands.

satellite payload constraints on volume, cost, mass and energy consumption, the radiometer uses a single mechanically scanned reflector antenna to collect radiation over a wide frequency range, from 23 GHz to 230 GHz. Within the MWS, it is therefore necessary to separate spectrally the linearly polarized TE or TM signals of the complete frequency range into five discrete bands.

The approach selected in the study [1], uses a quasi-optical feed train with four different FSS that are orientated at 45° to the direction of the wave propagation. Fig. 1 illustrates this frequency demultiplexing arrangement. The network design and performance is reported elsewhere [4]. It exploits a previously developed high performance FSS 1 [5]. We present here the design, manufacture and measured performance of the second demultiplexing element, FSS 2. This is technically the second most challenging FSS in the network because it is the only dichroic element which is required to simultaneously transmit both TE and TM waves in the resonant 50.2 – 57.7 GHz passband, and to reflect higher frequencies.

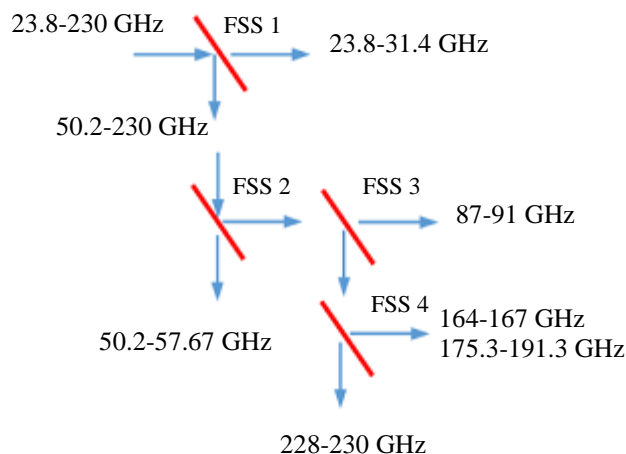


Fig. 1. MWS breadboard’s frequency demultiplexing scheme.

Table 1 presents the frequency, polarization and transmission/reflection requirements for FSS 2. Within each of these channels, the insertion loss specification is ≤ 0.25 dB in order to meet the instrumental requirements to achieve state of

the art receiver sensitivity and noise performance.

Table 1: Frequency, polarisation and operating mode requirements on the FSS

Channel frequency (GHz)	Frequency bandwidth (%)	Polarisation	Mode
54	13.9	TE & TM	Transmission
89	4.5	TM	Reflection
165.5	1.8	TE	Reflection
183.3	8.7	TE	Reflection
229	0.9	TE	Reflection

This paper describes the major advances that have been made to satisfy these stringent FSS specifications. Our design solution has been achieved by a synergy of innovative periodic array design and numerical optimization performed using a 3D electromagnetic simulator [6], development of state-of-the-art micromachining processes and spectral testing of the FSS using two different quasi-optical measurement systems [7, 8].

A critical requirement for this low-pass FSS is to exhibit coincident spectral responses for dual polarization excitation at 45° oblique incidence. In previously published work, several different low-pass, polarization independent, slot FSS suitable for use in Earth observation instrumentation have been reported [9, 10]. These structures were designed to meet the conflicting requirements of low-loss and fast spectral roll-off above resonance [11], to provide signal separation of two closely spaced narrow band frequency channels. In [12], dual polarized operation was obtained from a high-pass FSS composed of a periodic array of Jerusalem cross-slots which was designed to transmit radiation over a narrow band, 2 % wide, centered at 664 GHz. The spectral performance of the FSS design reported below differs significantly from these aperture element filter structures, and the requirements are much more challenging for three reasons, i) the FSS must exhibit a very much wider (14%) passband in transmission resonance, for both TE and TM polarisations, at 45° incidence, ii) grating lobes and signal leakage through the unit cell apertures, which are designed to resonate and generate a passband centered at 54 GHz, must be suppressed in order to obtain losses of ≤ 0.25 dB in channels from 89 GHz to 230 GHz for either TE or TM waves, and (iii) the FSS must operate over a max: min frequency ratio of 4.6:1. In addition, the FSS must be sufficiently robust to meet the structural, vibrational and thermal demands of spaceborne instrumentation.

The organization of the remainder of this paper is as follows. In section II the design and theory of operation is described along with the construction method for forming the periodic aperture elements. The computed spectral performance for an infinite array environment is presented. Section III describes

the key processing steps that were used to construct the FSS, including the creation of the highly conductive perforated metal screen, and the wafer bonding technique which was implemented to prevent the formation of voids between the superstrate and substrate. In Section IV quasi-optical transmission and reflection measurements are presented and discussed. Finally a summary of the work and conclusions are presented in Section V.

II. FSS DESIGN

The FSS structure consists of an array of 19,000 compact unit cells on a 100 mm diameter substrate. Each element composed of two nested slot resonators on a skewed grid, Fig. 2. The slots are formed in a metal layer which is sandwiched between two optically flat, 0.830 mm thick fused quartz substrates. A $10 \mu\text{m}$ thick layer of low loss glue (BCB), with electrical characteristics of $\tan\delta = 0.008$ and $\epsilon_r = 2.65$, is used to bond the two substrates together, forming a robust structure: Fig. 3. The glue layer has been simulated in the model to account for frequency shifts introduced by material changes at close proximity to the resonant slots, this improves the modelling accuracy. The metal is $3 \mu\text{m}$ thick copper, with a conductivity of 5.8×10^7 S/m, and the fused quartz layers have a permittivity $\epsilon_r = 3.78$ and loss tangent $\tan\delta = 0.004$. At 54 GHz, the passband center frequency, the combined electrical thickness of the quartz is selected to be $\lambda/2$, and therefore this provides a good impedance match to free space. The meandered λ elliptical shaped slots, Fig 2, are designed to resonate at 54 GHz and therefore to transmit corresponding signals with low insertion loss. A folded linear $\lambda/2$ dipole slot is inserted in the centre of each ellipse to achieve low loss in the lowest frequency reflection band, at 89 GHz. This second slot introduces a transmission resonance at 106 GHz which improves performance at 89 GHz on the basis that between any two resonant peaks there is an anti-resonance [13].

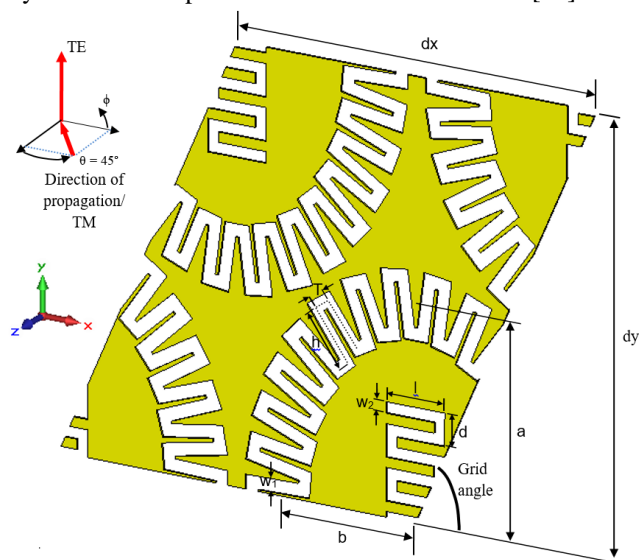


Fig. 2. FSS unit cell showing nested resonators on a skewed grid, the direction of propagation ($\theta = 45^\circ$, $\phi = 0^\circ$), and field orientations. Optimised design parameters (μm): $dx = 600$, dy

=690, $a = 335$, $b = 230$, $w_1 = 21$, $T = 24$, $h = 88$, $w_2 = 18$, $d = 52$, $l = 98$, grid angle = 66.5° .

The design dimensions were optimised to achieve the required low loss using the CST Microwave Studio frequency domain solver: Fig. 3. The numerical modeling included effects of the glue and metal thicknesses.

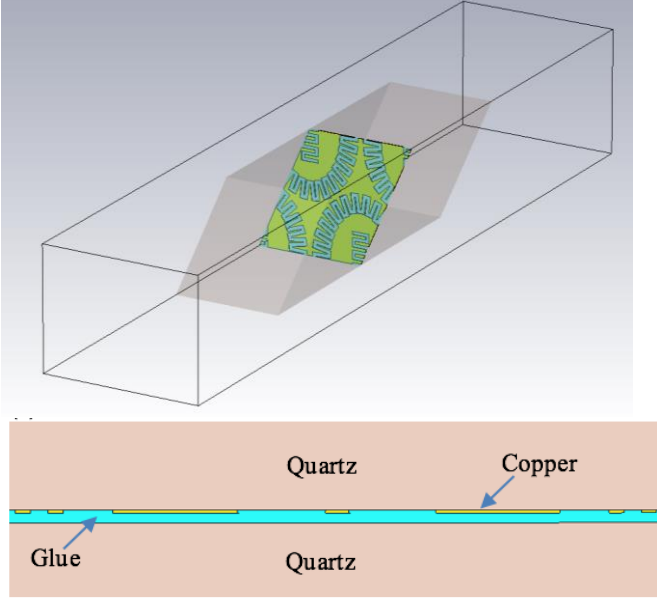


Fig. 3. Top: Unit cell as entered in CST for optimization and, bottom, indication of cross-section of the FSS.

Emphasis was placed on minimizing the unit cell periodicities in the x and y direction in order to suppress the appearance of grating lobes in the higher frequency reflection bands. This design strategy also increases the width of the passband and simultaneously reduces the sensitivity of the FSS to changes in incidence angle. The latter requirement is that performance is maintained over $\pm 2^\circ$, since the FSS is positioned at the network beam waist. Close packed array elements were achieved by meandering the resonators to make the unit cell more compact, by encasing the aperture elements in dielectric, and by skewing the grid. The two former features produced an 80% reduction in annulus diameter, when compared to free-space slots resonating at the same frequency.

To implement the convoluted elliptical slot design, a Matlab script was written to allow efficient control of the design parameters. The procedure started with a standard ellipse plotted as a series of x and y coordinates for $0 < \theta < 2\pi$:

$$x(\theta) = a \cos(\theta), \quad y(\theta) = b \sin(\theta) \quad (1)$$

θ is the angle relative to the centre of the ellipse, a and b are the semi-major and semi-minor axes of the ellipse respectively. The x , y positions of the centers of each of the meander cells were calculated. A large number ($N = 10000$) of linearly spaced values of θ were used, and the total length of the ellipse was approximated by summing the Euclidean distances between consecutive x , y coordinates:

$$length = \sum_{n=1}^{N-1} \sqrt{(x_n - x_{n-1})^2 + (y_n - y_{n-1})^2} \quad (2)$$

The meander cells were then equidistantly spaced around the circumference of the ellipse. The interpolation function in Matlab (`interp1`) was used to find the values of θ_m corresponding to the equidistantly spaced points. These values were entered into equations 1 and 2 to provide the x_m , y_m coordinates of each meander cell.

The centre line coordinates of the slot resonator were then calculated. The top and bottom edges of the meanders, of length T , were drawn at a tangent to the ellipse at each set of x_m , y_m coordinates. The tangent at each of these points was approximated as the tangent of a circle having a curvature that closely fits that of the local points on the curve. The radii of these circles were calculated using the radius of curvature:

$$R(\theta) = \frac{1}{|\kappa(\theta)|} \quad (3)$$

Where the curvature, κ , of the ellipse, was approximated at each point using:

$$\kappa(\theta) = \frac{ab}{(b^2 \cos^2(\theta) + a^2 \sin^2(\theta))^{3/2}} \quad (4)$$

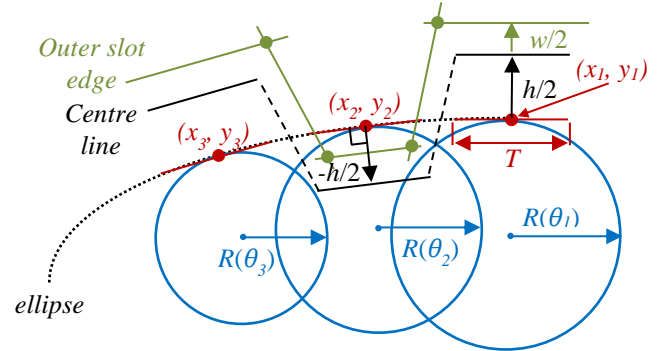


Fig. 4. Geometry and design of meandered elliptical slot resonator.

These straight edges were consecutively transformed by $h/2$ and $-h/2$ along their normal, where h is the length of the meander, and the ends of the consecutive transformed lengths were joined together to give the side edges of the meander centre line. The inner and outer edges of the slot resonator were then calculated by considering the meander centre line as a series of individual straight line segments. Each individual segment was transformed by $\pm w/2$ along the normal to that segment (where w is the resonator slot width). The interception points of the consecutive transformed lines were then used to provide the corners of the inner and outer edges of the slot, the latter of which is illustrated in Fig. 4. The x , y coordinates of the inner and outer slot edges were then exported as lists in text file format, which were imported into

CST using the polygon curve function. The remaining model geometry was drawn using CST standard CAD layout tools.

Fig. 5 depicts the predicted spectral transmission and reflection plots obtained after optimization of the dimensions of the unit cells. The results are illustrated from 20 – 230 GHz for both TE and TM signals in the transmission band (green) and four reflection bands (brown). Maximum predicted losses in each band are summarised in Table 2 in Section IV: the worst case loss is 0.18 dB at 89 GHz. The predicted performance of the FSS is therefore well within the 0.25 dB specification.

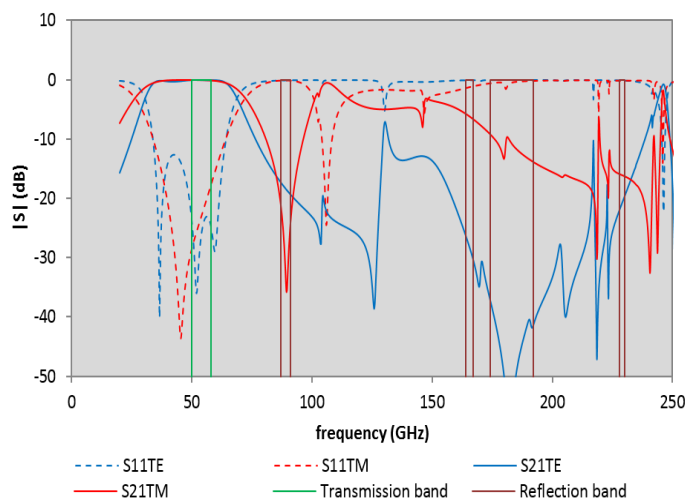
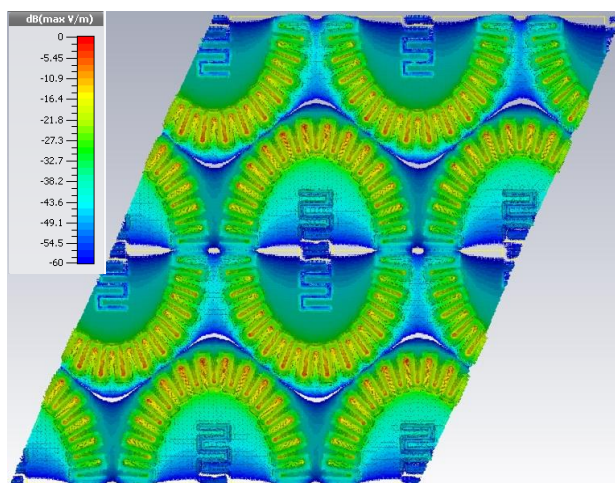
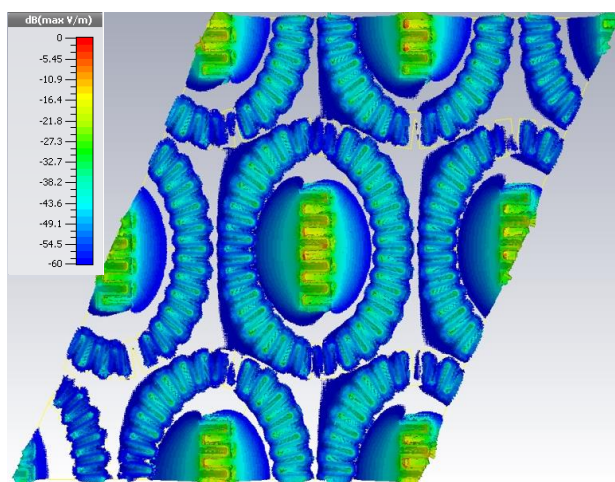


Fig. 5. Simulated spectral transmission (S_{21}) and reflection response (S_{11}) for the FSS at 45° incidence for TE and TM waves. The green and brown rectangles respectively show the transmission and reflection bands needed for the Microwave Sounder instrument.

To illustrate the FSS operation, Fig. 6 shows the computed surface electric fields at 54 GHz (TE) and 106 GHz (TM), corresponding to the λ and $\lambda/2$ resonances of the outer elliptical slot and the inner folded dipole, respectively. The effect of these resonances can be observed on the curves shown in Fig. 5. The 89 GHz reflection band, caused by an anti-resonance, lies between two TM peaks (red curve). In the design process the independent $\lambda/2$ slot dimensions were optimized to increase the depth of the 89 GHz transmission null. Fig. 7 shows the difference in the performance of the FSS around 89 GHz caused by the introduction of the folded $\lambda/2$ dipole. A reduction in the reflection loss of about 0.1 dB, to 0.26 dB, was thereby obtained.



(a)



(b)

Fig. 6. Computed resonant electric fields at the metal surface of the FSS for (a) 54 GHz TE polarization, when the elliptical slot is excited, and (b) for 106 GHz TM, which couples to the folded dipole.

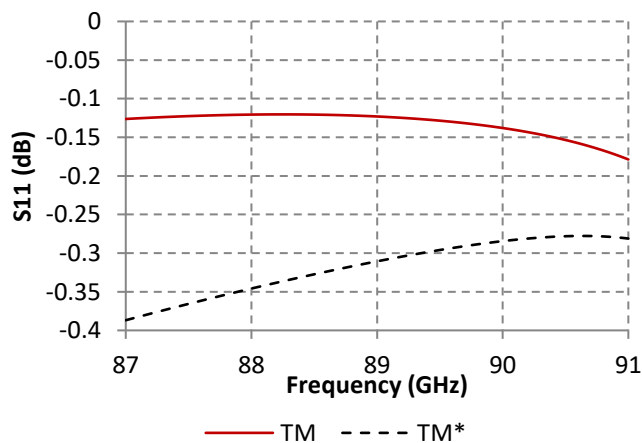


Fig. 7. Predicted TM reflection loss of the 89 GHz channel without (*dashed curve) and with (solid curve) the folded $\lambda/2$ slot dipole inserted in the unit cell.

III. MANUFACTURE

The FSS was fabricated using precision micromachining techniques in a cleanroom environment. Prior to processing, polished optically flat fused quartz substrates are matched in terms of their low bow and warp, $< 10 \mu\text{m}$, and are paired. The aperture elements are patterned on the surface of a metal layer deposited on the surface of one of the quartz substrates. The key manufacturing steps are shown in Fig. 8, and follow. Step 1: after cleaning, the quartz substrate is sputter coated, by DC magnetron sputtering, with a titanium 20 nm adhesion layer and a 250 nm copper layer. This copper layer provides a seed layer for high conductivity copper electroplating. Step 2: Prior to electroplating a $7 \mu\text{m}$ thick positive resist layer, AZ9260 is spun onto the quartz substrate and patterned using a UV exposure system. This transfers the element design onto the copper seed layer with the required manufacturing tolerance of $\pm 2 \mu\text{m}$. Step 3: Photolithography completed, a $4.5 \mu\text{m}$ copper layer is electroplated onto the exposed copper seed layer. The electroplating solution provides high conductivity copper with low stress. To improve the surface quality of the electroplated copper and to remove any copper islands (due to high current spots during electroplating), a surface polishing step is implemented. Step 4: A chemical mechanical polishing system is used to polish the metal. The polishing slurry is a mix of NH_4OH , $0.3 \mu\text{m}$ alumina abrasive and deionised water. The copper layer was reduced to a thickness of $3.5 \mu\text{m}$, leaving a flat copper surface with a RMS roughness of $< 150 \text{ nm}$. Once the copper is polished the resist pillars are removed in an ultrasonic solvent bath. Step 5: The original copper seed and titanium adhesion layers are subsequently chemically removed using controlled chemical etching solutions. Step 6: Cyclothen [14] benzocyclobutene (BCB) is used to form the adhesive layer between the quartz substrate containing the element design and the quartz superstrate. Ten microns of glue provides sufficient thickness at the interface, to fully bond across the complete surface when substrates with a similar flatness to the glue thickness are used. Thinner layers of glue were found to leave bond voids at the interface. Following spin coating of an adhesion promoter, a $10 \mu\text{m}$ BCB layer (5% uniformity) is spun onto the unpatterned quartz and partially cured at 120°C for 20 mins. The two quartz pieces are placed in contact ready for the bonding process. Step 7: The quartz/BCB/quartz assembly is placed between two polished metal plates in a customized vacuum bonding system. By bonding under vacuum, air voids that can be detrimental in a space environment and to the device's RF performance are prevented. The bond chamber was evacuated to a pressure of $\sim 6 \times 10^{-2} \text{ mbar}$. A pressure of 3.5 bar applied across the plates for 2 hours. In order to fully cure the BCB the bonded pair is heated to 250°C for a further 2 hours. After cooling to ambient, pressure on the bond plates is released and the chamber brought back to atmosphere.

A photograph of the polished copper surface of the FSS before BCB coating is shown in Fig. 9, along with the completed FSS in its holding bracket. This shows the closed packed nature of the elliptical outer and the inner linear slots. Dimensional characterization using an optical measurement method showed

that slot and periodic dimensions were typically within $2 \mu\text{m}$ of desired values. As a further verification, the mm-wave transmission of the patterned metal layer before bonding was also measured and compared with CST predictions.

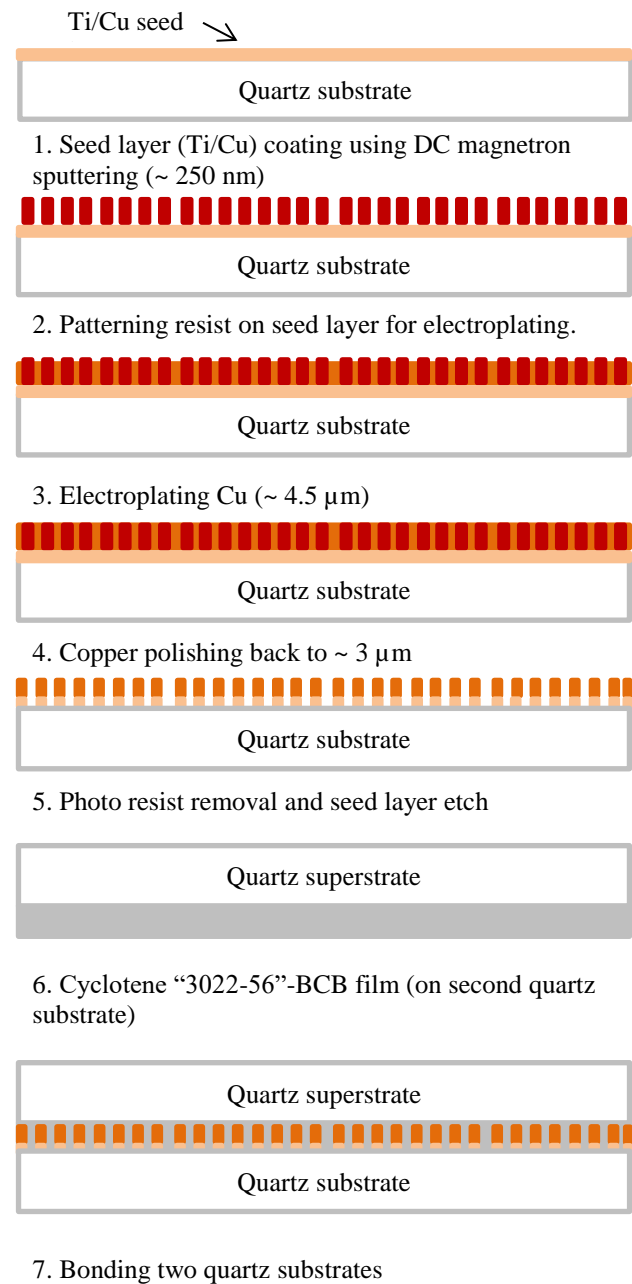


Fig. 8. Key steps in the FSS manufacture.

Preliminary environmental space qualification testing has been carried out on this type of FSS structure [5]. This involved thermal cycling in dry nitrogen, vibration testing including random and sine vibration. Inspection and full electromagnetic characterisation over the MWS channels before and after each series of applied stresses demonstrated that the FSS was not adversely affected.

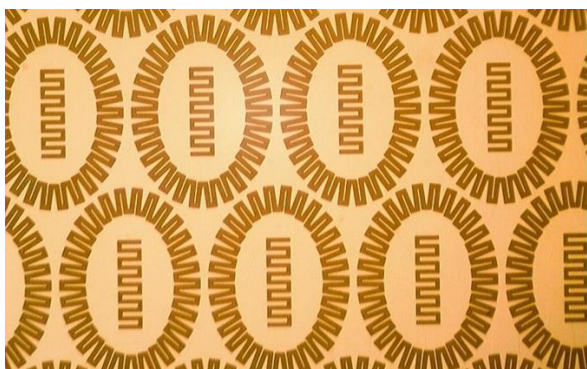


Fig. 9. Photographs (top) of the polished patterned copper on the quartz FSS substrate before attachment of the superstrate and (bottom) placeholder of the completed FSS in its mount.

IV. MEASURED RESULTS

The transmission and reflection coefficients of the manufactured FSS filter were measured at 45° incidence in the each of the five MWS instrument channels for both TE and TM polarisations. Measurement uncertainty is around 0.05 dB for transmission and reflection values very close to unity. For the two channels below 100 GHz, the measurements were made at Rutherford Appleton Laboratory using the quasi-optical bench shown in Fig. 10. For frequencies above 100 GHz, the FSS characterisation was performed at QUB, the quasi-optical test setup is shown in Fig. 11. Both test setups are based on quasi-optical free-space techniques to create a beam-waist at the position of the device under test (DUT) using components like mirrors, grids, horns etc. The horn and mirror design of the two quasi-optical test benches are optimised to work above (QUB) and below (RAL) 100 GHz, in order to provide plane wave illumination across the FSS in conjunction with the removal of truncation effects. Both setups use PNAs from different suppliers, the model numbers are given in the text wherever appropriate. The network used matched pairs of pyramidal horns and high gain ultra-Gaussian corrugated horns to cover the frequency bands 50-75 GHz and 75-100 GHz respectively. The feedhorns were aligned on the quasi-optical bench and connected to the Agilent PNA (Model numbers N5225A and E8361A for frequencies above and below 75 GHz respectively) and VDI millimetre wave modules (Model number N5262AW10 for 75-100 GHz measurements). The latter were fitted with

waveguide isolators to reduce standing wave effects. Residual impedance mismatches in, for example the feedhorns, leave a root mean square ripple of about 0.02 dB. A common set of four off-axis parabolic mirrors (M1-M4) and a pair of plane mirrors (P1, P2) were used to direct and focus the beam to produce a waist at the FSS position. Wire grid polarisers (G1, G2), set at 45° incidence, were introduced in both input and output beams just before and after the device under test (DUT), to ensure the beam polarisation purity for both reflection and transmission characterisation. A visible diode laser alignment system was used to ensure positional reproducibility during exchange of the DUT and its reference: this is particularly important for the reflection measurement.

The QUB test setup comprised an ABmm VNA (Model number MVNA-8-350-2) interfaced to a Thomas Keating [15] quasi-optical test bench: the reflection setup is shown in Fig. 11. It was configured to provide over 60 dB dynamic range and ± 0.05 dB signal uncertainty in the operating bands. The system consists of two identical broadband circularly symmetric corrugated feed horns connected to the transmitting and receiving ports of the VNA. The bench consists of a series of ellipsoidal mirrors that provide a highly focused Gaussian beam at the FSS sample position. At this position, a beam waist is formed, and the wave front can be considered plane wave.

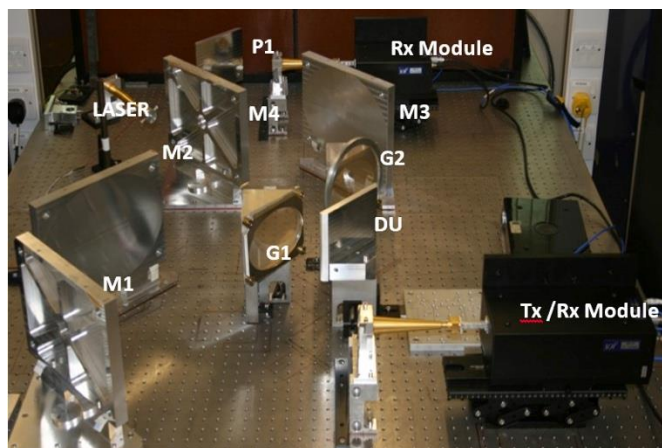


Fig. 10. Test setup for FSS reflectivity measurements, at frequencies below 100 GHz.

The largest beam is at the lowest frequency, 164 GHz, where the waist $\omega_0 = 9.33$ mm. At this frequency the edge illumination is very small, below -80 dB, therefore effects of the finite filter size can be ignored. For both RAL and QUB systems, a reference signal across the full waveguide band is obtained a) for transmission by inserting the empty FSS holder into the beam and b) for reflection by using a plane metal mirror in the place of the DUT in the FSS holder. Afterwards, the filter is introduced and S_{21} measurements made. The feedhorns and polarisers were then rotated by 90° and the measurements repeated for the orthogonal polarisation.

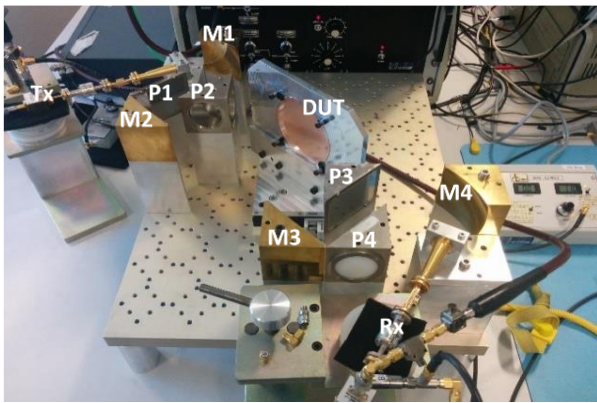
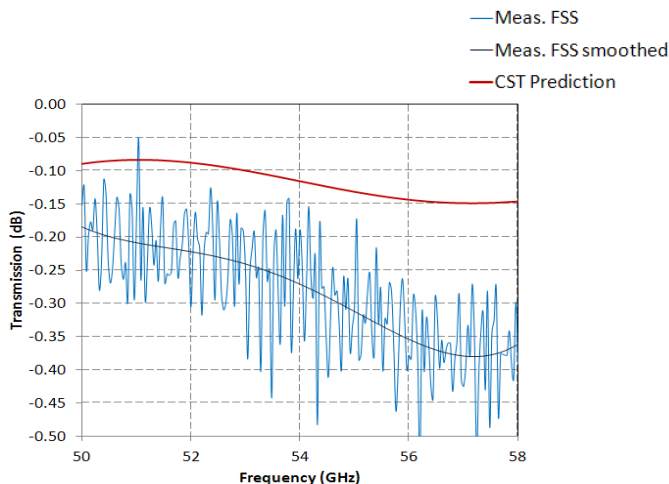


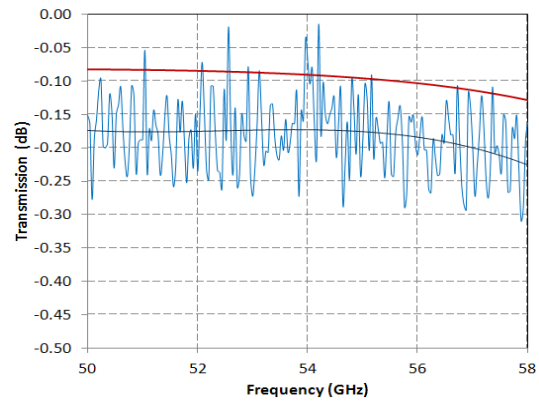
Fig. 11. Test setup for FSS reflection measurements at frequencies >100 GHz.

The FSS was mounted on a translation stage for reflectivity measurements, as it has been found that the effective reflecting plane is within the structure, and not at the front surface as for the metal reference reflector. The effects of unwanted reflections were reduced by applying a time gating procedure to the measured responses [16], (RAL set-up) and by placing absorbers in the beam path in the (QUB set-up) case. Time gating is a Fourier transform technique applied to reduce high frequency standing waves arising from undesired secondary reflections in the setup, such as slight mismatches from the horns and reference plate. Fig. 12 data shows how the application of time gating can remove the unwanted test set artefacts. In the QUB case, absorbers were effectively used to attenuate the secondary signals that reflect back and forth in the QO network.

The 50 – 58 GHz transmission measurements are shown in Fig. 12a, b. The filter generally exhibits the desired very high transmission for both TE and TM polarizations, with all losses less than 0.38 dB and 0.23 dB respectively. Measured insertion losses are slightly higher than the predictions, on average by about 0.15 dB for TE and 0.1 dB for TM. There is general good agreement between the trends of the predicted and measured curves.



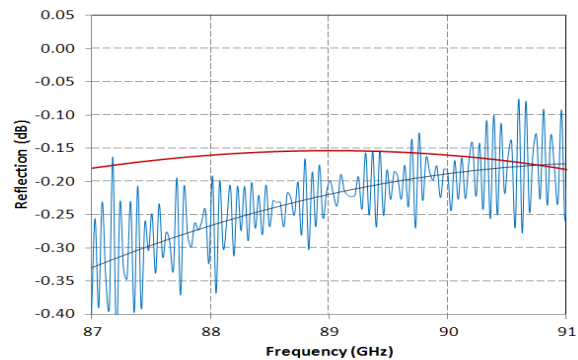
(a)



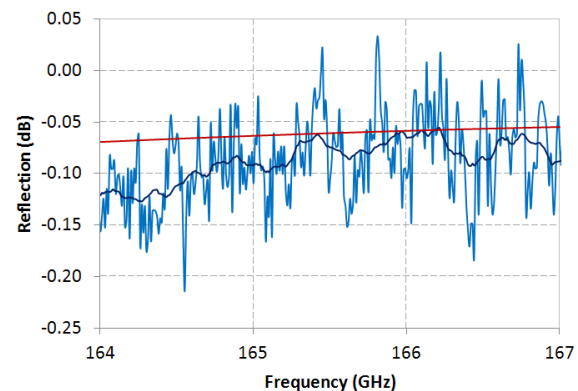
(b)

Fig. 12. Simulated (red) and measured (blue) transmission band measurements 50 - 58 GHz, (a) TE, (b) TM. The time gated averaged data are indicated by the smooth plotted dark blue line.

Reflection losses from the FSS are shown in Fig. 13 for each of the specified bands centered at 89, 165.5, 183 and 229 GHz. The maximum experimental losses are 0.33, 0.11, 0.13, and 0.22 dB respectively. In all cases, the measured losses are in very good agreement with predictions, with the largest discrepancy observed to be 0.15 dB at 89 GHz: Table 2.



(a)



(b)

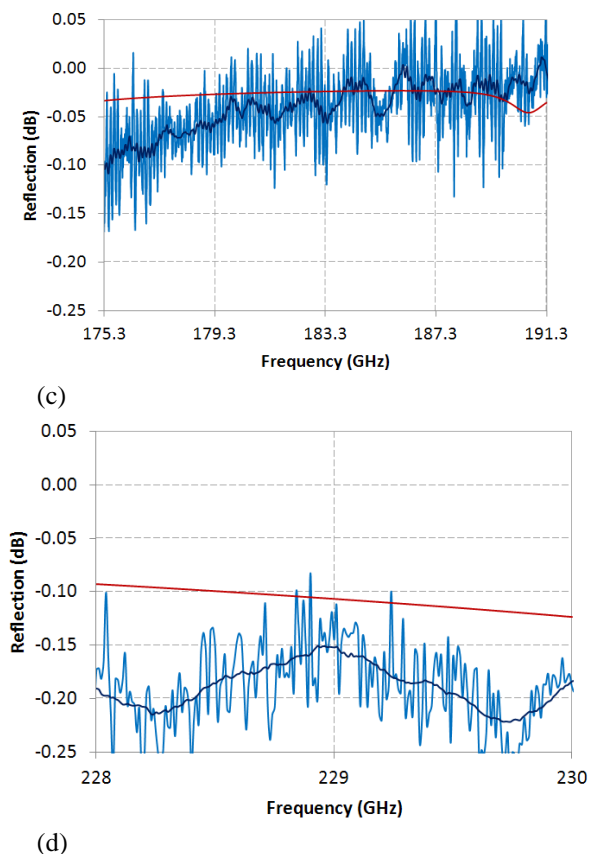


Fig. 13. Simulated (red) and measured (blue) reflection measurements in the specified bands centred at: (a) 89 GHz (TM), (b) 165.5 GHz (TE), (c) 183 GHz (TE), (d) 229 GHz (TE). The averaged data are indicated by the smoothed plotted dark blue line.

Commenting on the FSS measurements, the device meets the 0.25 dB performance specification in the MWS channels over the entire frequency range 50 - 230 GHz, apart from for TE polarisation in transmission between 53 and 58 GHz, where an excess loss of 0.13 dB is measured, and in TM reflection at the low frequency edge of the 89 GHz channel, where the loss is 0.08 dB higher than required.

Table 2: FSS insertion losses, requirements, predictions and measurement worst cases

Centre Frequency (GHz)	FSS Insertion Loss (dB)		
	Requirement	Prediction	Measurement
54 (TE)	≤ 0.25	0.14	0.38 +/- 0.05
54 (TM)	≤ 0.25	0.14	0.23 +/- 0.05
89 (TM)	≤ 0.25	0.18	0.33 +/- 0.05
165.5(TE)	≤ 0.25	0.07	0.11 +/- 0.05
183.3(TE)	≤ 0.25	0.05	0.13 +/- 0.05
229(TE)	≤ 0.25	0.12	0.22 +/- 0.05

V. CONCLUSIONS

We have developed an ultra-wide band FSS design that works from 50 – 230 GHz and exhibits low loss, between 0.11 dB – 0.38 dB, across the five frequency bands of the MWS instrument. A novel method of nesting two slot resonators in each unit cell has been implemented to provide coincident TE and TM spectral responses and improved insertion loss performance in the first reflection band centered at 89 GHz. The FSS manufacturing technique is based on bonding optically flat low loss fused quartz substrates combined with a high conductivity patterned metal sandwich layer. This approach provides high mechanical strength and rigidity for the construction of large arrays of shaped elements, such as meandered annular and linear slots, which are reported in this paper. The construction method has excellent thermal and mechanical stability needed for its demanding operating environment, as demonstrated by successful preliminary qualification tests [5]. Although the maximum measured losses of this FSS are slightly higher than the specifications in two bands, the overall performance of the quasi-optical system was maintained by performance improvements achieved in other FSS [1, 5]. Precision spectral transmission and reflection measurements, made independently at QUB and RAL are in good agreement with simulated results and confirm that the design and manufacturing techniques are suitable for meeting the stringent electromagnetic (and environmental) requirements for the MWS instrument.

REFERENCES

- [1] M. Candotti, R. Donnan, O. Sushko, C. Parini, R. Dubrovka, P. G. Huggard, M. Henry, K. Parow-Souchon, M. Oldfield, R. Dickie, R. Cahill, P. Baine, V. Fusco, V. Kangas, and M. van der Vorst, “MetOp Second Generation Microwave Sounder Instrument: Part 1 – Quasi-Optical and Microwave Components’ Design”, in preparation for IEEE TAP.
- [2] V. Kangas, S. D’Addio, M. Betto, H. Barre and G. Mason, “MetOp second generation microwave radiometers,” *Microwave Radiometry and Remote Sensing of the Environment (MicroRad)*, ESA, The Netherlands, pp. 1-4, March 2012.
- [3] V. Kangas, C. Lin and M. Betto, “Microwave Instrument Requirements and Technology Needs for the Post-EPS Mission,” *Proc 31st ESTEC Antenna Workshop on Millimetre and sub-millimetrewaves - From technologies to systems*, The Netherlands, European Space Agency, pp. 501 -506, May 2009.
- [4] Pre-Development of Quasi-Optical Network For the Microwave Sounder of MetOP-SG, Report, ESTEC Contract No. 4000107540/13/NL/BJ.
- [5] R. Dickie, R. Cahill, P. Huggard, M. Henry, V. Kangas, P. de Maagt: “Development of a 23-230 GHz FSS for the MetOP Second Generation Microwave Sounder Instrument”, *Proc 7th European Conference on Antennas and Propagation, EUCAP 2013, Gothenburg, Sweden, April 2013*.
- [6] CST Microwave Studio, [Online]. Available: <https://www.cst.com/Products/CSTMWS>
- [7] Keysight Technologies: Millimeter Wave Frequency Extenders, [Online] <http://literature.cdn.keysight.com/litweb/pdf/59913161EN.pdf?id=2395009>
- [8] AB Millimetre, [Online]. Available: <http://www.abmillimetre.com>
- [9] R. Dickie, R. Cahill, V. F. Fusco, H. S. Gamble, B. Moyna, P. Huggard, N. Grant and C. Philpot, “300GHz high Q resonant slot frequency selective surface filter,” *Proc. IET Microwaves Antennas and Propagation*, vol. 151, pp. 31-36, Jan 2004.
- [10] R. Dickie, R. Cahill, H. S. Gamble, V. F. Fusco, M. Henry, M. L. Oldfield, P. G. Huggard, P. Howard, N. Grant, Y. Munro, and P. de Maagt, “Submillimetre wave frequency selective surface with

polarisation independent spectral responses,” *Proc IEEE Antennas and Propagation*, vol. 57, pp. 1985 – 1994, July 2009.

- [11] R. Dickie, R. Cahill, H. Gamble, V. Fusco, and N. Mitchell, “THz frequency selective surface filters for Earth observation remote sensing instruments,” *IEEE Trans. Terahertz Science and Technology*, vol. 1, no. 2, pp. 450 – 461, Nov. 2011.
- [12] R. Dickie, R. Cahill, N. Mitchell, H. Gamble, V. Fusco, and Y. Munro, “664 GHz dual polarization frequency selective surface,” *Electron. Lett.*, vol. 46, no. 7, pp. 472–474, Apr. 2010.
- [13] B. A. Munk, *Frequency Selective Surfaces Theory and Design*. New York: Wiley, 2000.
- [14] The Dow Chemical Company, [Online]. Available: <http://www.dow.com/cyclotene/prod/302257.htm>
- [15] Thomas Keating, [Online]. Available: <http://www.terahertz.co.uk/>
- [16] “Time Domain Analysis Using a Network Analyzer”, Agilent application note 1287-12 [Online] <http://cp.literature.agilent.com/litweb/pdf/5989-5723EN.pdf>



Raymond Dickie received a BEng honors degree in Electrical and Electronic Engineering in 2001 from Queen’s University Belfast. From 2001 – 2004 he worked on an Astrium industrially funded project specialising in frequency selective surfaces, and received his PhD from Queen’s University Belfast in 2004. In October 2004 he joined the high frequency electronic circuits and antennas group at The Institute of Electronics, Communications and Information Technology (ECIT) in Belfast where he is now employed as a Principal Engineer developing mm-wave technology for the space and communication industries. His work on freestanding frequency selective surfaces has been patented and includes design and fabrication methods. Dr Dickie has experience in photolithographic processing and working in clean room environments where he develops MEMS devices. Dr Dickie has coauthored over 60 publications, his high frequency research interests include numerical modeling of high frequency structures and precision quasi-optical measurements in the millimeter and sub millimeter wave bands.



Steven Christie is the lead antenna designer at Arralis Technologies Ltd. He received the MEng honors degree in Electrical and Electronic Engineering in July 2009, and a Ph.D in High Frequency Electronic Circuits in July 2013, from Queen’s University Belfast. He is currently working on development of mm-wave beam-forming networks for radar and communications systems, and miniaturised multi-band antennas using high impedance surfaces for GNSS and communications, and has 2 international patent applications pending.



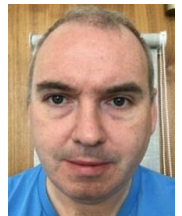
Robert Cahill (M’10–SM’11) received a BSc honors degree in Physics from the University of Aston in Birmingham in 1979 and a PhD degree in microwave electronics from the University of Kent at Canterbury in 1982. He joined Queen’s University Belfast (QUB) in 1999 after a 17 year career working in the UK space and defense industry, where he worked on antenna and passive microwave device technology projects. During this time he pioneered methods for predicting the performance of antennas on complex scattering surfaces such as satellites and has developed techniques for analyzing and fabricating mm and sub-mm wave quasi-optical dichroic filters. Recently he has established a 100 - 700 GHz quasi-optical S parameter measurement facility at QUB. He has exploited the results of numerous research

projects, sponsored by the European Space Agency, EADS Astrium Space Ltd, the British National Space Agency, the Centre for Earth Observation Instrumentation (CEOI) and the UK Meteorological Office, to develop quasi-optical demultiplexers for atmospheric sounding radiometers in the range 89-500 GHz. These include AMSU-B, AMAS, MARSCHALS and the ESA 500GHz demonstrator. Dr Cahill’s recent interests also include the characterization of liquid crystal materials at microwave and mm wavelengths, and strategies for broad banding and creating active reflectarray antennas. He has (co) - authored over 130 publications and holds 4 international patents.

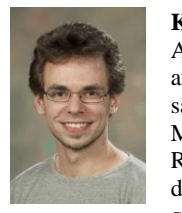


Vincent Fusco FREng, IEEE Fellow (2004), FIET, FIAE, MRIA. In 2012 he was awarded the IET senior achievement award the Mountbatten Medal for seminal contributions in the field of microwave electronics and its impact on UK industry. His fundamental work on active antenna front-end techniques has provided generic advances in low cost phased and self-tracking antenna array architectures.

This work has strongly impacted advanced system concepts in areas requiring communications between un-stabilized platforms and is enabling the next generation of mobile terrestrial to satellite broadband internet connectivity. He has written over 450 papers and two books and holds a number of antenna related patents. He is presently the CTO of the major research institute in electronics and information technology ([ECIT](#)) at Queens University Belfast.



Dr P Baine graduated from the Queen’s University Belfast with a first class Beng honours degree in Electrical and Electronic Engineering in 1992. In 1997 he received the PhD degree for his research in the area of single crystal silicon on glass for display applications. The title of his dissertation was “ Fabrication of Thin Single Crystal Silicon Devices on Glass Using Electrostatic Bonding” . Paul has been with Queen’s University Belfast since 1994 working on research activities involving SOI, Silicon Bonding, the bonding of non-standard materials and buried-silicide GPSOI structures and Germanium on Sapphire. More recently he has been involved in LC filled reflectarray fabrication and FSS fabrication for ESA. He currently holds the role of Manager of the Queen’s Advanced Micro-Engineering Centre, responsible for the operation of a high class semiconductor and nanotechnology fabrication laboratory as well as providing support for ongoing research contracts. Other areas of expertise include: wafer processing technology, photolithography and device fabrication.



Kai Parow-Souchon graduated from RWTH Aachen University in Germany in October 2014, after studying electronic engineering with focus on satellite communications. He then joined the Millimetre Wave Technology Group at the STFC Rutherford Appleton Laboratory and worked on the design and near field scanning test of a breadboard quasi-optical network for ESA’s Microwave Sounder (MWS) instrument. He is currently working on millimeter wave amplifier modules and other RF components to be used in the three millimetre wave instruments in ESA’s MetOp operational meteorology programme: MWS, MWI and ICI. Kai’s additional research interest is the development of diode based THz power detector modules.



Manju Henry obtained her Masters and PhD degree in Electronic Engineering from Cochin University of Science and Technology, Kerala, India in 1998 and 2002 respectively. After her PhD, she had done five years of post-doctoral studies at Institute of High Frequency and Microwave Techniques (IHM) at Karlsruhe Institute of Technology, the former FZK,

Germany and at University of Surrey, UK. She joined the Millimetre Wave Technology Group at STFC Rutherford Appleton Laboratory in 2007. After joining the group she had undertaken key technical and management roles in several EU/ESA programs. She is currently involved in a wide range of tasks that include millimetre wave passive system design for atmospheric sounding and astronomy, active system development for meteorological remote sounding and security imaging. She was awarded the Senior Research Fellowship (SRF) by the Council of Scientific and Industrial Research, Govt. of India, New Delhi during her PhD. She has more than 75 publications in international journals/conferences.

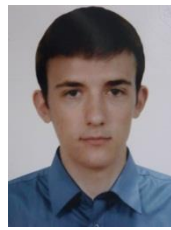


Peter Huggard (SM'12) Peter Huggard received BA(Mod) in Experimental Physics and PhD degrees from the University of Dublin, Trinity College in 1986 and 1991 respectively. Since 2000, Dr Huggard has been a member of the Millimetre Wave Technology Group in the UK's STFC Rutherford Appleton Laboratory. He is now a UK Research Councils Individual Merit Fellow and deputy leader of the Group. Dr Huggard's interests include developing photonics sources and semiconductor diode based receivers for GHz and THz radiation, the characterisation of frequency selective surfaces, and the calibration of mm wave radiometers. He has contributed to 50 refereed journal articles and a similar number of conference proceedings.



Robert S. Donnan BSc, MSc, PhD, CPhys, FInstP, FIET, graduated in mathematical physics from the University of Wollongong, NSW, Australia (1990); the University of Technology, Sydney, with a Masters in Applied Physics (1995); and completed a PhD in solid state physics from the University of Wollongong in 2000. He joined Queen Mary

University of London in 2001 as a research assistant in the Antennas & Electromagnetics Group of the Department of Electronic Engineering. He was appointed a lecturer in 2003, promoted to senior lecturer in 2013 and to Reader in Terahertz Engineering Physics in 2015. He founded the terahertz metrology laboratory within the School of Electronic Engineering & Computer Science in 2009 that develops and applies methods of antenna metrology to the life sciences broadly and to basic and applied research in millimetre-wave and THz engineering specifically. He is a Fellow of the Institute of Physics, a Fellow of the Institute of Engineering and Technology, UK, and a Chartered Physicist and general committee member of the Instrument Science and Technology Group of the UK Institute of Physics.



Oleksandr Sushko graduated with honors MSc degree in radio-engineering from National Technical University of Ukraine "Kyiv Polytechnic Institute" in 2010. He received his Ph.D. degree titled "Terahertz dielectric study of bio-molecules using time-domain spectrometry and molecular dynamics simulations" from Antennas and Electromagnetics group at Queen Mary University of London in 2014. He then

continued working in the same group as a postdoctoral research assistant, first on development of mm-wave components for new generation of space-borne sounder for meteorological satellite, then on development of quasi-optical sub-THz sources based arrays of Schottky diodes. His research interests include THz materials characterization and liquid spectroscopy, mm-wave and THz antennas and components, quasi-optical circuits and their applications.



Rostyslav Dubrovka PhD, MSc, MBA, MIET, MIEEE graduated as a radio engineer from the National Technical University of Ukraine "Kyiv Polytechnic Institute" in 1993. Then, in 2000 he received his PhD from the same institution. In 1997 he became an Executive Manager of a small Research & Development company in Kyiv, Ukraine, continuing his research activity. He joined the Antenna & Electromagnetics Group at Queen Mary University of London in February

2001 as a post-doctoral research assistant. In 2006 he became an Antenna CAD/CAM Engineer and in 2014 – Terahertz and Quasi-Optics Research Lab Manager. From 1991 to 2000 his research covered area of mm-wave slot antenna arrays, microwave planar devices, including optically controlled active elements, finite aperture antenna arrays and feed systems for various reflector systems of various size and configurations, including 5 and 7 m hub stations, VSAT antennas, radio-relay reflector antennas, etc. Since 2001 his research has covered compact corrugated horns, new equivalent circuit method for design of frequency selective surfaces, methods of analysis for on-body propagation, low-mass low-profile antenna arrays for air-borne synthetic aperture radars, modelling techniques and applications of metamaterials for mm-wave quasi-optical earth observation radiometers, wire media applications for antennas, design of quasi-optical networks for new generation of space-borne sounders for meteorological satellites and THz spectroscopy for life sciences. Currently, he is a principal investigator of the EPSRC funded project on Active Quasi-optics for Power THz Science. He is a co-inventor of five patents on feed systems for satellite communications. He is a reviewer of several world leading conferences and journals on antennas and microwave devices including IEEE TAP/MTT, IET MAP, Electronic Letters, EuCAP, etc.



Clive G. Parini BSc (Eng), PhD, CEng, FIET, MIEEE, FREng Joined Queen Mary University of London as Lecturer in 1977, promoted to Reader in 1990, promoted to Professor in 1999 and is currently Professor of Antenna Engineering and heads the Antenna & Electromagnetics Research Group. He has published over 450 papers on research topics including array mutual coupling, array beam forming, antenna metrology,

microstrip antennas, millimetrewave compact antenna test ranges, millimetrewave integrated antennas, metamaterials and on-body communications. In 2008 he co-authored the book entitled "Principles of Planar Near-Field Antenna Measurements", and in 2014 the book entitled "Theory and Practice of Modern Antenna Range Measurements". He is a Fellow of the IET and a past

Chairman of the IET Antennas & Propagation Professional Network Executive Team. He was a member of the editorial board till Jan. 2015 and past Honorary Editor for the IET Journal *Microwaves, Antennas & Propagation*. In 2009 he was elected a Fellow of the Royal Academy of Engineering.



Ville Kangas received the M.Sc. (Tech.) degree from the Helsinki University of Technology, Finland. From 2000 to 2002 he was working at Helsinki University of Technology, Laboratory of Space Technology developing an aircraft radiometer. From 2002 to 2003 he was working on antenna testing at European Space Agency (ESA). From 2003-2006 he was working as Microwave Design engineer at Ylinen Electronics involved in development of SMOS radiometer and TerraSAR-L radar. From 2006 to 2007 he was a project manager at Elektrobit Ltd developing a mobile base station product. Since 2007 he has been with European Space Agency (ESA). From 2007 to 2012 he was working on ESA future radiometer developments for earth observation. Since 2013 he has been with MetOp Second Generation project and its radiometers. He has authored and coauthored more than 50 publications in the area of microwave instruments, technology and remote sensing. His research interest include microwave instruments, technology and related spacecraft systems.